The role of a conserved tyrosine in the 49-kDa subunit of complex I for ubiquinone binding and reduction. Biochim Biophys Acta

ARTICLE *in* BIOCHIMICA ET BIOPHYSICA ACTA · JUNE 2010

Impact Factor: 4.66 · DOI: 10.1016/j.bbabio.2010.01.029 · Source: PubMed

6 AUTHORS, INCLUDING:

Maja Aleksandra Fedorowicz
Columbia University
16 PUBLICATIONS **1,007** CITATIONS
SEE PROFILE

Stefan Dröse
Goethe-Universität Frankfurt am Main
76 PUBLICATIONS **3,684** CITATIONS
SEE PROFILE

Biochimica et Biophysica Acta 1797 (2010) 625–632

Contents lists available at ScienceDirect

Biochimica et Biophysica Acta

journal homepage: www.elsevier.com/locate/bbabio

The role of a conserved tyrosine in the 49-kDa subunit of complex I for ubiquinone binding and reduction

Maja A. Tocilescu, Uta Fendel, Klaus Zwicker, Stefan Dröse, Stefan Kerscher, Ulrich Brandt *

Molecular Bioenergetics Group, Medical School, Cluster of Excellence Frankfurt "Macromolecular Complexes", Center for Membrane Proteomics, Johann Wolfgang Goethe-Universität, Frankfurt am Main, Germany

ARTICLE INFO

Article history:
Received 23 November 2009
Received in revised form 7 January 2010
Accepted 25 January 2010
Available online 1 February 2010

Keywords:
Mitochondria
Complex I
Ubiquinone
Inhibitor resistance
Mutagenesis
Yarrowia lipolytica

ABSTRACT

Iron–sulfur cluster N2 of complex I (proton pumping NADH:quinone oxidoreductase) is the immediate electron donor to ubiquinone. At a distance of only ~7 Å in the 49-kDa subunit, a highly conserved tyrosine is found at the bottom of the previously characterized quinone binding pocket. To get insight into the function of this residue, we have exchanged it for six different amino acids in complex I from *Yarrowia lipolytica*. Mitochondrial membranes from all six mutants contained fully assembled complex I that exhibited very low dNADH:ubiquinone oxidoreductase activities with *n*-decylubiquinone. With the most conservative exchange Y144F, no alteration in the electron paramagnetic resonance spectra of complex I was detectable. Remarkably, high dNADH:ubiquinone oxidoreductase activities were observed with ubiquinones Q_1 and Q_2 that were coupled to proton pumping. *Apparent* K_m values for Q_1 and Q_2 were markedly increased and we found pronounced resistance to the complex I inhibitors decyl-quinazoline-amine (DQA) and rotenone. We conclude that Y144 directly binds the head group of ubiquinone, most likely via a hydrogen bond between the aromatic hydroxyl and the ubiquinone carbonyl. This places the substrate in an ideal distance to its electron donor iron–sulfur cluster N2 for efficient electron transfer during the catalytic cycle of complex I.

1. Introduction

Mitochondrial complex I (NADH:ubiquinone oxidoreductase) is a large membrane protein and the least understood component of the respiratory chain [1–3]. It is composed of at least 40 subunits with a total mass of ~1 MDa [4,5]. In contrast to other respiratory chain complexes, a complete crystal structure of complex I has not been solved yet. However, single particle electron microscopy revealed that complex I has an L-shaped overall structure in eukaryotes as well as in prokaryotes [6–10]. The hydrophobic membrane domain of the enzyme is embedded in the inner mitochondrial membrane, whereas the hydrophilic peripheral domain protrudes into the mitochondrial matrix. Interestingly, the peripheral domain contains all known redox centers: one non-covalently bound FMN and 8–9 iron–sulfur clusters [11–14]. In contrast, no redox centers were found in the membrane domain of complex I [15]. However, this part of the enzyme must harbor the proton pumping machinery.

The mechanism by which complex I couples the redox reaction of NADH oxidation and quinone reduction to the translocation of four protons across the inner mitochondrial membrane [16,17] is still unknown. However, from recent results it seems that the reduction of quinone in the peripheral domain induces long range conformational changes in the membrane domain, which result in proton uptake at the matrix side of the inner mitochondrial membrane and proton release into the intermembrane space [3,18,19].

Previously, we suggested that the quinone and inhibitor binding pocket is located at the interface of the PSST and the 49-kDa subunit [20,21] (the bovine nomenclature for homologous complex I subunits will be used throughout). This suggestion was based on several observations. Firstly, the active site of water-soluble [NiFe] hydrogenases is located at the interface of the small and large subunits which are evolutionary related to the PSST and the 49-kDa subunit as indicated by sequence comparison [22,23]. Secondly, mutagenesis studies showed that many functionally critical residues are located in the PSST and the 49-kDa subunit and that mutations which target the former [NiFe] site conferred resistance towards complex I inhibitors which act at the quinone binding site [20,24–29]. Thirdly, photoaffinity labeling studies suggested that the PSST subunit forms part of

Abbreviations: ACMA, 9-amino-6-chloro-2-methoxyacridine; BN-PAGE, blue-native polyacrylamide gel electrophoresis; $C_{12}E_8$, n-alkyl-polyoxyethylene-ether; DBQ, *n*-decylubiquinone; dNADH, deamino-nicotinamide-adenine-dinucleotide (reduced form); DQA, 2-decyl-4-quinazolinyl amine; EPR, electron paramagnetic resonance; FCCP, carbonyl-cyanide-*p*-trifluoromethoxyphenylhydrazone; HAR, hexa-ammine-ruthenium(III)-chloride; Hepes, 4-(2-hydroxyethyl)-1-piperazineethanesulfonic acid; log*P*, decadic logarithm of the partition coefficient; Mops, 3-(*N*-morpholino) propanesulphonic acid; PMSF, phenylmethylsulfonyl fluoride; Q_1, ubiquinone-1 (2,3-dimethoxy-5-methyl-6-(3-methyl-2-butenyl)-1,4-benzoquinone); Q_2, ubiquinone-2 (2,3-dimethoxy-5-methyl-6-geranyl-1,4-benzoquinone); Q_9, ubiquinone-9; Tris, Tris (hydroxymethyl)aminomethane

* Corresponding author. Universität Frankfurt, Zentrum der Biologischen Chemie, Molekulare Bioenergetik, Theodor-Stern-Kai 7, Haus 26, D-60590 Frankfurt am Main, Germany. Tel.: +49 69 6301 6926; fax: +49 69 6301 6970.
E-mail address: brandt@zbc.kgu.de (U. Brandt).

0005-2728/$ – see front matter © 2010 Elsevier B.V. All rights reserved.
doi:10.1016/j.bbabio.2010.01.029

the quinone and inhibitor binding pocket of complex I [30]. Further support came from subsequent mutagenesis studies, which identified additional functionally important residues in the PSST and 49-kDa subunit [31–33] and recent photoaffinity labeling studies which showed that the 49-kDa subunit forms part of the inhibitor binding site of complex I [34]. Finally, the crystal structure of the hydrophilic domain of complex I from *Thermus thermophilus* at 3.3 Ångström resolution [14] confirmed our proposal. The structure revealed the spatial arrangement of seven central hydrophilic subunits as well as the locations of all known redox centers of complex I. Seven iron–sulfur clusters (N1b, N2, N3, N4, N5, N6a und N6b) form an approximately 95 Å long chain of redox centers. This chain starts with iron–sulfur cluster N3 next to the FMN molecule in the 51-kDa subunit, continues via the redox centers of the 75-kDa and the TYKY subunits and ends at iron–sulfur cluster N2 in the PSST subunit adjacent to a broad cavity at the interface of the PSST and the 49-kDa subunit, which corresponds to the suggested quinone reduction domain.

Taking advantage of our model organism, the strictly aerobic yeast *Yarrowia lipolytica*, we exchanged all amino acid residues located at the surface of this large cavity. Subsequent structure/function analysis allowed the identification of functional domains [35]. A possible ubiquinone access path leading from the N-terminal β-sheet of the 49-kDa subunit into the cavity to a tyrosine residing next to iron–sulfur cluster N2 was identified. Within the cavity many amino acid residues were found to be critical for oxidoreductase activity of complex I. In a more recent study, we used the large array of mutations targeting the quinone binding pocket to identify the binding sites of different complex I inhibitors [36]. The obtained results suggested that type A, B and C inhibitors [37] indeed bind to the quinone binding pocket at the interface of the PSST and the 49-kDa subunit and that the binding sites overlap spatially, as had been deduced from earlier competition experiments [38].

According to the crystal structure of the hydrophilic domain of complex I from *T. thermophilus* [14], Y144 (*Y. lipolytica* numbering) of the 49-kDa subunit is located only ~7 Å away from iron–sulfur cluster N2, the immediate electron donor to ubiquinone (Fig. 1). This tyrosine is highly conserved between prokaryotes and eukaryotes (Fig. 2). The side chain of Y144 seems to define the border between the PSST subunit coordinating iron–sulfur cluster N2 and the 49-kDa subunit forming most of the quinone binding pocket. By systematically exchanging this tyrosine to aromatic, hydrophilic and hydrophobic amino acids, we show here that this residue is critical for ubiquinone binding and reduction in complex I.

2. Materials and methods

2.1. Materials

Asolectin (total soy bean extract with 20% lecithin) was purchased from Avanti Polar Lipids (Alabaster, AL), *n*-dodecyl-ß-D-maltoside from Glycon (Luckenwalde, Germany), and octyl-ß-D-glucopyranoside from Biomol (Hamburg, Germany). 9-amino-6-chloro-2-methoxyacridine (ACMA) was obtained from Invitrogen/Molecular Probes (Eugene, OR) and decylubiquinone (DBQ) from Alexis Biochemicals (Lausen, Switzerland). DQA (2-n-decyl-quinazolin-4-yl-amine, SAN 549) was from AgrEvo (Frankfurt, Germany). Carbonyl-cyanide-*p*-trifluoromethoxyphenylhydrazone (FCCP) and the ionophore valinomycin were from Sigma. ACMA, DBQ, Q_1, Q_2, DQA, roteonone, and the ionophores were dissolved in dimethylsulfoxide.

2.2. Site-directed mutagenesis

Site-directed mutagenesis, preparation of mitochondrial membranes, determination of protein concentration, and structural image preparations were performed as described in [35].

2.3. Analytical methods

Measurement of NADH:HAR and dNADH:DBQ oxidoreductase activities was performed as described [35]. Inhibitor insensitive activities were determined in the presence of 27 µM DQA. *Apparent* K_m and V_{max} values for DBQ, Q_1 and Q_2 were measured as described for dNADH:DBQ oxidoreductase activity [35] except that the concentrations of DBQ, Q_1 or Q_2 were adjusted to the respective ranges and that DQA was omitted. A DQA insensitive rate could not be determined because the concentrations needed to completely block complex I would have been too high for the mutant strains (see Results). Instead, background rates determined in parallel with mitochondrial membranes of the *Δnucm* strain were subtracted from the rates measured with the parental and mutant strains in the absence of inhibitor. Since the *Δnucm* strain does not contain complex I, these background rates that were in the same range as the inhibitor

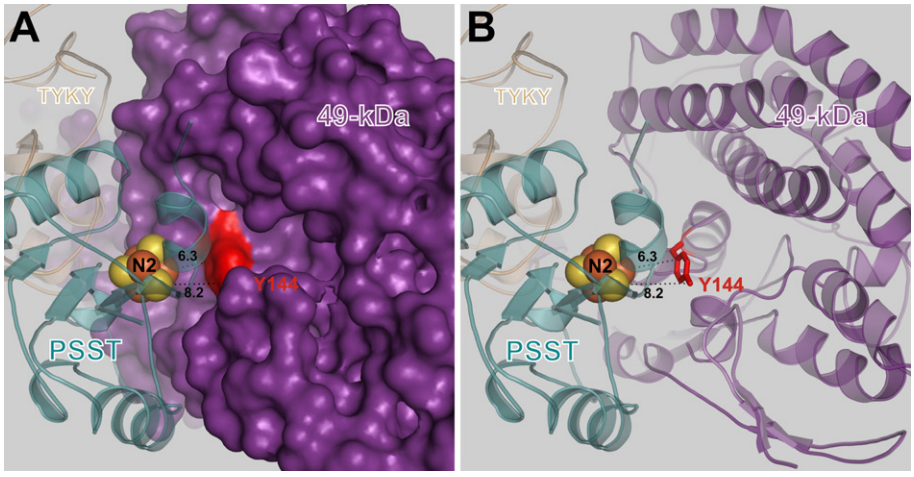

Fig. 1. Y144 from the 49-kDa subunit is located between iron–sulfur cluster N2 and the quinone binding pocket. The PSST, the 49-kDa and the TYKY subunits are colored in cyan, purple and beige, respectively. Y144 is highlighted in red. Iron–sulfur cluster N2 is depicted as spheres. Numbers give center-to-center distances between atoms in Ångström. The figure was prepared with the PyMol software package (version 0.99) using the coordinates from the crystal structure of the hydrophilic domain of complex I from *T. thermophilus* (2FUG). A, Surface representation of the 49-kDa subunit is shown in order to visualize the quinone binding pocket. B, Cartoon representation of the 49-kDa subunit showing the side chain of Y144.

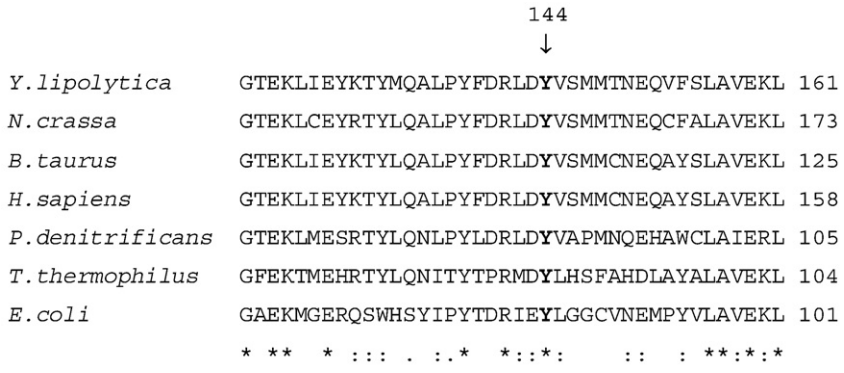

Fig. 2. Sequence alignment of the 49-kDa subunit harboring the highly conserved Y144. NCBI sequences of *Y. lipolytica* (CAG78336), *Neurospora crassa* (CAA38368), *Bos taurus* (P17694), *Homo sapiens* (AAC27453), *P. denitrificans* (P29916), *T. thermophilus* (AAA97941) and *E. coli* (CAA48363) were aligned by the multiple sequence alignment program ClustalW. Invariant (*), highly (:) and weakly similar (.) positions are labeled.

insensitive rates were considered as complex I unspecific. Data were fitted to the Michaelis–Menten equation using the Enzfitter software package, and the value for substrate concentration [S] was corrected as described earlier [39]. To obtain comparable maximal activities for different strains, the V_{max} values were normalized to complex I content of the respective mitochondrial membrane preparations.

I_{50} values were determined in the presence of 180 μM Q_1 as the concentration needed to inhibit 50% of the initial rate minus the insensitive rate that was determined at the maximal concentration of the respective inhibitor. In the case of DQA and rotenone, the insensitive rate for the parental strain was also used for membranes from the mutant strains, because maximal inhibition was not reached due to pronounced inhibitor resistance.

Samples for EPR were reduced by NADH. It is not necessary to use dNADH for reduction of membrane samples because NDH-2 does not contain any paramagnetic cofactors which might contribute to the EPR spectrum. EPR spectroscopy was performed as described in [35]. All other parameters are given in the figure legends. BN-PAGE was performed as described in [40].

2.4. Preparation of complex I and proteoliposomes

Complex I was purified as described previously [41] with two minor modifications: (i) after ultracentrifugation the supernatant was adjusted to 55 mM imidazole and pH 7.4. (ii) the imidazole concentration for equilibration and washing of the Ni-NTA fast flow Sepharose column was reduced from 65 mM to 55 mM.

Complex I proteoliposomes were prepared from purified complex I as described in [42] with minor modifications as detailed in [43]. Proton pumping by complex I proteoliposomes was determined by ACMA quench as described previously [42].

3. Results

3.1. Complex I assembly but no dNADH:DBQ oxidoreductase activity in Y144 mutants

In order to gain insight into the function of Y144 we changed it to phenylalanine and tryptophan retaining the aromatic character, to the hydrophobic isoleucine and to the hydrophilic amino acids histidine, serine and arginine. Mutant Y144H has been described before [20], however it was characterized in a different genetic background at the time and was therefore generated and analyzed again here.

Mitochondrial membranes were isolated from the tyrosine mutants and complex I content was estimated as NADH:HAR oxidoreductase activity (Table 1). In mutants Y144I and Y144R complex I content was moderately reduced to ~60% and in mutant Y144W it was increased to ~130%. Within experimental error, mutants Y144F, Y144H and Y144S exhibited unchanged amounts of complex I. These results were confirmed by BN-PAGE followed by complex I in-gel activity staining (data not shown). Apparently, Y144 was not essential for complex I assembly and/or stability, but spacious hydrophobic or hydrophilic residues were less well tolerated than aromatic residues at this position.

Measurement of specific dNADH:DBQ oxidoreductase activities revealed that all mutations resulted in a drastic reduction in complex I activity (Table 1). Notably, this was also true for Y144F, the mutant where just the aromatic hydroxyl group had been removed. Even concentrations of DBQ up to 140 μM corresponding to ~10 times the *apparent* K_m of the parental strain or variation of the pH value or addition of varying concentrations of different anions that could have potentially served as proton-carriers in proteins (chloride, bromide, iodide, azide, formate or acetate) did not stimulate complex I activity in mitochondrial membranes from mutant Y144F (data not shown). Remarkably, when we measured the dNADH oxidase activity to probe for the activity of the entire respiratory chain via the endogenous substrate Q_9, we also found very low activities (Table 1).

Table 1
Effects of point mutations of Y144 in the 49-kDa subunit on complex I content, activity and iron–sulfur cluster N2 EPR signal in mitochondrial membranes from *Y. lipolytica*.

Strain	Complex I content[a]	Complex I activity[b]	dNADH oxidase activity[c]	N2 EPR signal (see EPR spectra below)
	%	%	%	
Parental	100 ± 3	100 ± 5	100	Reference
Y144F	110 ± 2	15 ± 2	5	Not altered
Y144W	129 ± 2	11 ± 4	<5	N2 signal slightly shifted
Y144I	59 ± 1	12 ± 1	<5	No N2 signal
Y144H	86 ± 2	5 ± 3	<5	N2 signal slightly shifted
Y144S	94 ± 4	13 ± 1	n.d.	Reduced N2 signal
Y144R	58 ± 1	8 ± 1	n.d.	No N2 signal

n.d., not determined.

[a] 100% of complex I content corresponds to 1.25 μmol min^{-1} mg^{-1} NADH:HAR oxidoreductase activity determined for the parental strain. Mean values ± SEM are given.

[b] Specific complex I activity was determined as dNADH:DBQ oxidoreductase activity from which the insensitive rate in the presence of 27 μM DQA of the parental strain (0.06 μmol min^{-1} mg^{-1}) was subtracted. The activities were normalized to complex I content and the activity of the parental strain (0.46 μmol min^{-1} mg^{-1}) was set as 100%. Mean values ± SEM are given.

[c] In order to determine specific dNADH oxidase activities by probing the entire respiratory chain via endogenous Q_9 the insensitive rate in the presence of 27 μM DQA of the parental strain (0.04 μmol min^{-1} mg^{-1}) was subtracted for each strain. The activities were normalized to complex I content and the activity of the parental strain (0.12 μmol min^{-1} mg^{-1}) was set as 100%.

3.2. Iron–sulfur cluster N2 in Y144 mutants

Since Y144 is only ~7 Å away from iron–sulfur cluster N2 (Fig. 1), mutations of this tyrosine could have abolished complex I activity by interfering with this cluster. To test this, EPR spectra of mitochondrial membranes from Y144 mutant strains were recorded. As shown in Fig. 3 and summarized in Table 1, the EPR signals of iron–sulfur cluster N2 in mutants Y144F, Y144W and Y144H were, if at all, only slightly changed when compared to the parental strain. Mutant Y144S displayed clear changes in a region where mainly the g_z and the g_{xy} signals of iron–sulfur cluster N2 contributed to the spectrum. In mutants Y144I and Y144R no cluster N2 EPR signals were visible. Mutant Y144W revealed some shift of signals to lower field in the g_{xy} region of cluster N2. This was also visible in the N2 spectrum derived from purified enzyme (Fig. 4), but the g_z signal seemed unchanged.

Mutant Y144H had been shown previously to display a slight shift in the signal of iron–sulfur cluster N2 [20]. Since small changes in the EPR signals of iron–sulfur cluster N2 cannot be detected in mitochondrial membranes, complex I from mutants Y144F and Y144W was purified for a more detailed EPR analysis. However, in standard EPR spectra recorded at 12 K no changes were evident in the signatures of iron–sulfur cluster N2 in purified complex I from mutant Y144F (data not shown). By subtracting EPR spectra recorded at 40 K that show only signals of the slow relaxing 2Fe–2S cluster N1 from spectra recorded at 25 K that show signals from N1 and the 4Fe–4S cluster N2, essentially pure spectra of iron–sulfur cluster N2 were obtained (Fig. 4). In these spectra the g_{xy} signal of iron–sulfur cluster N2 was shifted slightly towards lower field in mutant Y144W. In mutant Y144F however, the EPR signature of cluster N2 was unchanged, indicating that the environment of iron–sulfur cluster N2 was not affected significantly by removing the hydroxyl group of Y144.

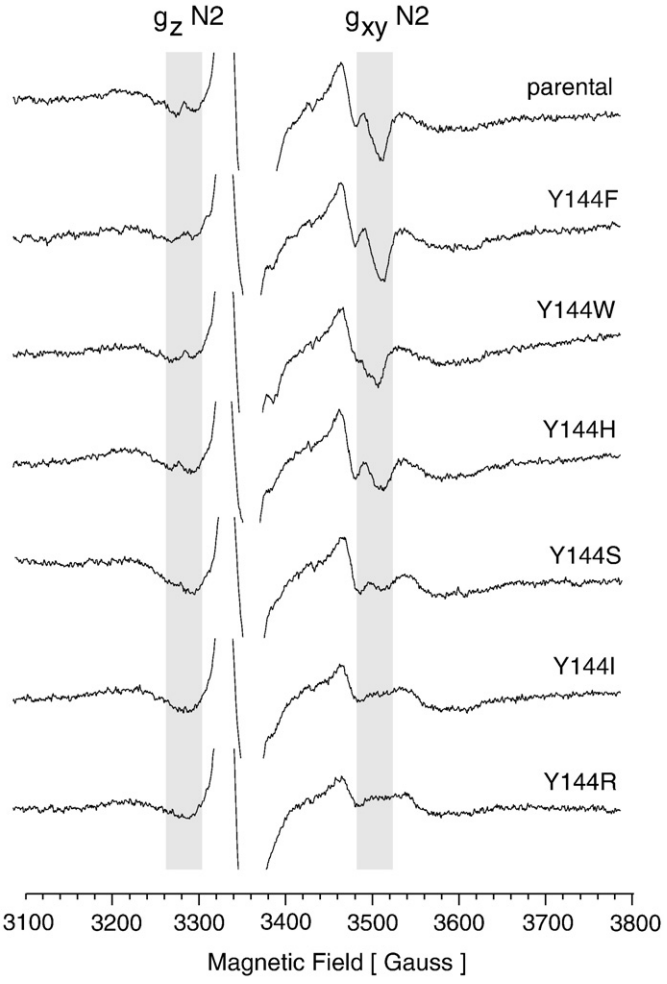

Fig. 3. EPR signals of iron–sulfur cluster N2 in Y144 mutants. EPR spectra were recorded from mitochondrial membranes at 12 K and 5 mW microwave power. Field regions where signals originated predominantly from cluster N2 are highlighted in gray. Y144F, Y144W and Y144H showed, if at all, only minor changes when compared to the parental strain. In Y144S significant changes in N2 signals were observed, whereas in Y144I and Y144R no iron–sulfur cluster N2 derived signals were detected. The prominent signal at 3340 G in all spectra was due to oxidized iron–sulfur cluster S3 of complex II. For sample preparation, mitochondrial membranes (25 mg protein per ml) were reduced by 2 mM NADH.

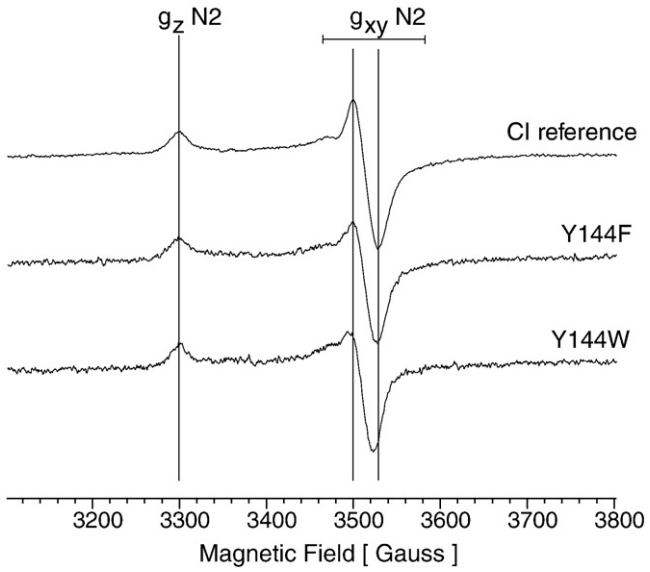

Fig. 4. EPR spectra of iron–sulfur cluster N2 in complex I from mutants Y144F and Y144W. 25 K minus 40 K difference EPR spectra from purified complex I of mutants Y144F and Y144W were compared to a highly concentrated complex I reference. Vertical lines indicate minima and maxima from the g_z and the g_{xy} signals of iron–sulfur cluster N2. In contrast to mutant Y144F, a small shift of the g_{xy} signal of iron–sulfur cluster N2 was evident for mutant Y144W. Original 40 K and 25 K EPR spectra were recorded at 2 mW microwave power from samples reduced with 5 mM NADH.

Overall, the effects of the tyrosine mutations on the EPR signal of iron–sulfur cluster N2 are in excellent agreement with the close proximity of this residue to cluster N2. Consistent with their destabilizing effect on complex I, mutations Y144I and Y144R completely abolished the EPR signal of cluster N2 (Fig. 3; Table 1). In contrast, mutation Y144F did not interfere with iron–sulfur cluster N2 at all, indicating that the near complete loss of complex I activity in this mutant was not due to changes in the environment of iron–sulfur cluster N2.

3.3. dNADH:Q_1 oxidoreductase activities and apparent K_m values

It has been reported that the reactivity of ubiquinone derivatives with complex I depends on the properties of their isoprenoid or aliphatic side chains [44–48]. Therefore, we also tested our mutants with the more hydrophilic Q_1 carrying one isoprenoid moiety as a side chain that is also frequently used as electron acceptor in routine assays of complex I.

We assayed the activity with Q_1 as electron acceptor in mutants Y144F, Y144W and Y144H. In these mutants the environment of iron–sulfur cluster N2 was, if at all, only slightly altered (Fig. 4; [20]). In contrast to the measurements with DBQ, we observed considerable dNADH:Q_1 oxidoreductase activities and could thus determine Michaelis–Menten parameters for this substrate. As shown in Table 2, mutant Y144F reached more than 70% and mutant Y144W reached more than 90% of the maximal dNADH:Q_1 oxidoreductase activity of the parental strain. Mutant Y144H reached 48% of parental

Table 2
Apparent K_m and *V_{max}* values for Y144 mutants with Q_1 as electron acceptor.

Strain	*Apparent K_m* for Q_1	*V_{max}* for Q_1 normalized to CI content[a]	
	μM	μmol min^{-1} mg^{-1}	%
Parental	9 ± 1	0.29 ± 0.01	100 ± 3
Y144F	54 ± 7	0.21 ± 0.01	72 ± 3
Y144W	130 ± 30	0.27 ± 0.06	93 ± 21
Y144H	180 ± 60	0.14 ± 0.04	48 ± 14

Mean values ± SEM.
[a] The *V_{max}* values were normalized to complex I content in mitochondrial membranes that was estimated as NADH:HAR oxidoreductase activity.

strain activity. These values are remarkable considering that hardly any activity was detectable for these mutants with DBQ (Table 1). The *apparent K_m* value for Q_1 was six times higher in mutants Y144F and even about fourteen times higher when Y144 was exchanged to the bulkier tryptophan in mutant Y144W. With mutant Y144H the *apparent K_m* value could hardly be determined, but was at the order of 20 times the value of the parental strain.

3.4. dNADH:Q_2 oxidoreductase activities and apparent K_m values

We then measured dNADH:Q_2 oxidoreductase activities in mitochondrial membranes from mutants Y144F and Y144W and determined the Michaelis–Menten parameters for Q_2. As shown in Table 3, the normalized *V_{max}* values for both mutants were similar to the values determined for Q_1 and in mutant Y144W this parameter was essentially identical to the parental strain. However, the *apparent K_m* values had only doubled relative to the parental strain. Thus, in comparison to the values determined for Q_1, the changes in the *apparent K_m* value for Q_2 were much less pronounced. We conclude that in mitochondrial membranes from the Y144 mutants Q_2 was an even better substrate than Q_1.

In summary, the dNADH:ubiquinone oxidoreductase activities and *apparent K_m* values in mitochondrial membranes from the Y144 mutants strongly depended on the structure of the side chain of the ubiquinone derivative used.

3.5. Proton pumping by complex I from mutant Y144F

Since mutant Y144F displayed high oxidoreductase activities with Q_1 and Q_2 as substrates, we next tested whether this redox reaction was linked to vectorial proton pumping by complex I and thus, whether these ubiquinone derivatives were reduced at the physiological site. For this purpose, purified complex I from mutant Y144F was reconstituted into proteoliposomes and proton pumping was monitored as quench in ACMA fluorescence. As indicated by the fluorescence quench upon addition of NADH (Fig. 5), complex I from mutant Y144F exhibited proton pumping activities with all three ubiquinone derivatives. The ACMA traces quite well reflected the differences in electron transfer activities observed with the different substrates that were quite similar in membranes and for the enzyme reconstituted into proteoliposomes. While the decay in fluorescence for complex I from Y144F was very slow with DBQ, the traces with Q_1 and Q_2 were comparable for parental and mutant complex I. In contrast to parental complex I however, the ACMA quench was reverted only partially upon addition of 10 μM of the complex I inhibitor DQA. This reflected the pronounced resistance of mutant Y144F for this inhibitor (see below). Complete restoration of the ACMA fluorescence to the level prior to the addition of NADH was achieved by addition of the protonophor FCCP.

The finding that all dNADH:ubiquinone oxidoreductase activities of the tyrosine mutant were linked to proton pumping indicated that these activities reflected the physiological reaction. Moreover, these results highlight the tight coupling between redox reaction and vectorial proton pumping in complex I.

Table 3
Apparent K_m and *V_{max}* values for Y144 mutants with Q_2 as electron acceptor.

Strain	*Apparent K_m* for Q_2	*V_{max}* with Q_2 normalized to CI content[a]	
	μM	μmol min^{-1} mg^{-1}	%
Parental	7 ± 1	0.31 ± 0.01	100 ± 3
Y144F	11 ± 2	0.23 ± 0.03	74 ± 10
Y144W	14 ± 2	0.32 ± 0.03	103 ± 10

Mean values ± SEM.
[a] The *V_{max}* values were normalized to complex I content in mitochondrial membranes that was estimated as NADH:HAR oxidoreductase activity.

3.6. Inhibitor resistance

Since the dNADH:Q_1 oxidoreductase activity of complex I in mutant Y144F was coupled to proton translocation and thus Q_1 reduction clearly occurred at the physiological site, we tested whether exchanges of Y144 affected inhibitor binding at the quinone binding pocket. We determined I_{50} values for DQA, rotenone and $C_{12}E_8$ as representatives of all three classes of complex I inhibitors. As shown in Table 4, removal of the hydroxyl group of Y144 by the Y144F exchange was sufficient to induce an almost 1000-fold resistance towards DQA and a 3.7 fold resistance towards rotenone. Even higher resistance was observed when the tyrosine was exchanged for the larger tryptophan. The dramatic increase of the I_{50} values for DQA in both mutants suggested that Y144 is a critical component of the binding site for this inhibitor. In contrast, rotenone binding seemed to be less directly affected by the mutations. Remarkably, both mutants exhibited a slight hypersensitivity for $C_{12}E_8$, as has been observed for a number of other mutants in the ubiquinone binding pocket [36]. Note however that the rate that could not be inhibited even at very high concentrations of $C_{12}E_8$ was markedly higher in both mutants (not shown). Overall, these results lend further support to the idea that complex I contains a large quinone binding pocket with distinct but overlapping binding sites for the three types of inhibitors [38].

4. Discussion

We show that the conserved Y144 of the 49-kDa subunit of complex I is directly involved in the binding of the substrate ubiquinone. This is consistent with its central position within the quinone binding pocket only ~7 Å away from iron–sulfur cluster N2, the immediate electron donor to ubiquinone ([14,35]; Fig. 1). Exchanging this tyrosine with a series of six different amino acids did not prevent complex I assembly; however, in all cases the dNADH:DBQ oxidoreductase activity of complex I was drastically reduced. This was also true for complex I from mutant Y144F in which only the hydroxyl group of Y144 was missing. While in all other mutants changes in the EPR signature of the nearby iron–sulfur cluster N2 ranged from a slight shift to complete loss of the signal, no effect was seen in mutant Y144F. This excluded structural changes in the environment or the loss of the electron donor for ubiquinone as reasons for the decreased catalytic activity. Rather, it seemed that a critical binding interaction was lost in the mutant, with a hydrogen bond between the tyrosine-hydroxyl and a carbonyl of the ubiquinone head group being the most obvious option.

When we tested the activities with the short chain isoprenoid derivatives Q_1 and Q_2, complex I from mutants Y144F and Y144W exhibited high ubiquinone reductase activities that for Y144W reached the level of the parental strain (Tables 2 and 3). However, significant changes in the *apparent K_m* that were much more pronounced in the case of Q_1 suggested that also binding of these ubiquinone derivatives was affected. We conclude that the isoprene moieties, most likely through hydrophobic and π–π interactions of their double bond, contributed significantly to substrate binding,

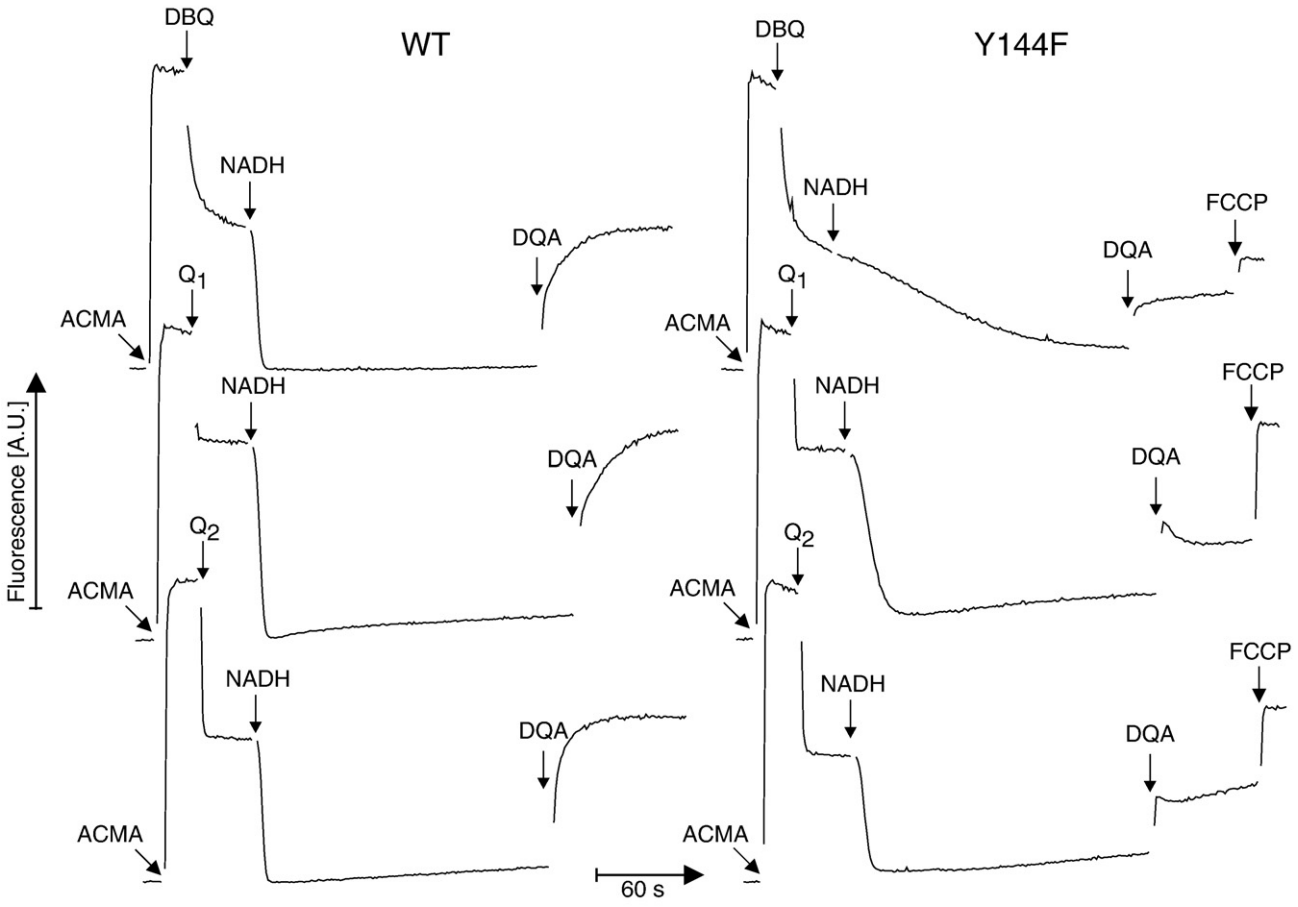

Fig. 5. Proton pumping by proteoliposomes containing complex I from the parental strain and mutant Y144F. In the presence of 60 μM DBQ, Q_1 or Q_2, the addition of NADH resulted in the buildup of a proton gradient across the membrane of the proteoliposomes that was monitored as a quench of ACMA fluorescence. Addition of the complex I inhibitor DQA reverted this quench, however in the case of mutant Y144F only addition of the protonophore FCCP returned the signal back to the level prior to NADH addition. The line shapes of the ACMA fluorescence signal for the mutant with Q_1 and Q_2 were comparable to those of the parental strain, indicating that this mutation did not interfere with proton pumping. Even with DBQ as substrate some ACMA fluorescence quench was observed. Proteoliposomes containing ~20 μg of complex I were added to 2 ml buffer (20 mM K^+/Mops pH 7.2, 80 mM KCl, 0.5 μM valinomycin) in a stirred cuvette. H^+-translocation was monitored as fluorescence change of ACMA that was added to a final concentration of 0.5 μM. Measurements were performed in a Shimadzu RF-5001 fluorimeter at an excitation wavelength of 430 nm and an emission wavelength of 475 nm (band pass 5 nm each, integration time 1 s) at 30 °C. Arrows indicate time points for the additions of 60 μM ubiquinone derivative, 100 μM NADH, 10 μM DQA and 1 μM FCCP.

thereby restoring catalytic activity. The large increase in the *apparent* K_m value for Q_1 in the case of mutant Y144W may indicate that in addition to the loss of the hydrogen bond, the bulky tryptophan may have distorted the binding site, weakening the binding interaction with the isoprenoid moiety. The reduced effect of the two mutations on the *apparent* K_m for Q_2 suggests that also the second isoprene-residue made binding interactions with complex I, thereby further reducing the effect of abolishing the hydrogen bond with Y144.

One may infer that an increasing number of binding interactions should also result in a corresponding decrease of the K_m values for the different ubiquinone derivatives in the parental strain. However, this correlation is difficult to assess because only *apparent* K_m values could be measured that do not take into account the different hydrophobicity of the substrates that are likely to affect the effective concentration at the binding site. If one considers the membrane/water log*P* values [46] of 4.7 for DBQ, 2.9 for Q_1 and 4.0 for Q_2, it becomes clear that also this parameter cannot be applied in a straightforward way. Consistent with the proposed difference in the number of binding interactions, an *apparent* K_m of 15 μM for DBQ and of 9 μM for Q_1 indeed seems to suggest a much weaker binding of DBQ if one takes into account that the difference in the partition coefficient is almost two orders of magnitude. However, this argument does not hold if one compares Q_1 and Q_2, because the higher log*P* and the assumed additional binding interaction for Q_2 together would have suggested a much larger difference in the *apparent* K_m values than was actually observed. This may suggest that the exact position and interactions of the ubiquinone side chains may depend on the length and steric properties of the side chain. Indeed, it has been known for a long time that short chain ubiquinones exhibit some degree of substrate inhibition in complex I from bovine heart [46,48] and *P. denitrificans* [49,50] suggesting a different mode of binding as compared to long chain ubiquinones, the physiological substrates of complex I. Moreover, specific binding of the quinone isoprenyl side chain by complex I was demonstrated earlier [51]. Notably, we found for the three mutants still containing essentially normal amounts of iron–sulfur cluster N2 that the dNADH oxidase activities employing the physiological substrate Q_9 were even lower than the dNADH:DBQ oxidoreductase activities (Table 1). It is tempting to speculate that this could also suggest different binding modes of the first two isoprenoid

Table 4
I_{50} values for DQA, rotenone and $C_{12}E_8$ determined in mitochondrial membranes from tyrosine mutants in the presence of Q_1.

Strain	I_{50}		
	DQA	Rotenone	$C_{12}E_8$
	nM	nM	nM
Parental	10	950	3000
Y144F	9500	3500	1500
Y144W	14,000	7000	1500

units for long and short chain quinones resulting in a weaker interaction with the quinone binding pocket of complex I near Y144 for the longer variants. Because it is technically difficult to add larger amounts of the extremely hydrophobic endogenous substrate Q_9 to mitochondrial membranes, we could not test whether higher concentrations would have increased the activity. Therefore, the question whether a distorted orientation of the isoprenoid double bonds or a specific folding of the side chain of the long chain ubiquinone within the binding pocket are responsible for the low activities of the mutant complexes with the physiological substrate has to remain unanswered at this point.

In summary, our results clearly show that the aromatic hydroxyl group of tyrosine 144 is directly involved in binding the substrate, but not required for efficient electron transfer. Understanding the detailed interaction of the ubiquinone derivatives with complex I will require further studies.

Remarkably, mutations Y144F and Y144W also resulted in drastic resistance to DQA, suggesting that this inhibitor also binds directly to this tyrosine qualifying it as a true quinone analog. The inhibitory efficiencies of rotenone and $C_{12}E_8$ were only moderately altered, suggesting that the binding of these compounds was affected only indirectly by the mutations. This is consistent with the idea of a large binding pocket with distinct but overlapping inhibitor binding sites [36,38].

Based on structural studies with the peripheral arm of *T. thermophilus* complex I, it has been proposed recently that Y144 (Y87 in *T. thermophilus*) of the 49-kDa subunit may act as a proton-donor and may be involved in ubiquinone protonation or a possible direct proton pumping mechanism [52]. This seems highly unlikely based on our finding that complex I from mutant Y144F, after reconstitution into proteoliposomes, pumped protons efficiently when Q_1 or Q_2 were used as substrates. Our results clearly demonstrate that redox linked proton pumping was functional in complex I from mutant Y144F and that the hydroxyl group of Y144 was not required for substrate protonation or proton pumping.

We conclude that Y144 directly binds the head group of ubiquinone most likely via a hydrogen bond between the aromatic hydroxyl and the quinone carbonyl. This places the substrate in an ideal distance to its electron donor iron–sulfur cluster N2 for efficient electron transfer during the catalytic cycle of complex I.

Acknowledgements

We would like to thank Gudrun Beyer, Andrea Duchene and Ilka Siebels for excellent technical assistance. This work was supported by the Deutsche Forschungsgemeinschaft EXC115 and SFB 472, Project P2.

References

[1] U. Brandt, Energy converting NADH:quinone oxidoreductase (complex I), Annu. Rev. Biochem. 75 (2006) 69–92.
[2] V. Zickermann, S. Dröse, M.A. Tocilescu, K. Zwicker, S. Kerscher, U. Brandt, Challenges in elucidating structure and mechanism of proton pumping NADH: ubiquinone oxidoreductase (complex I), J. Bioenerg. Biomembr. 40 (2008) 475–483.
[3] V. Zickermann, S. Kerscher, K. Zwicker, M.A. Tocilescu, M. Radermacher, U. Brandt, Architecture of complex I and its implications for electron transfer and proton pumping, Biochim. Biophys. Acta 1787 (2009) 574–583.
[4] J. Carroll, I.M. Fearnley, J.M. Skehel, R.J. Shannon, J. Hirst, J.E. Walker, Bovine complex I is a complex of 45 different subunits, J. Biol. Chem. 281 (2006) 32724–32727.
[5] N. Morgner, V. Zickermann, S. Kerscher, I. Wittig, A. Abdrakhmanova, H.D. Barth, B. Brutschy, U. Brandt, Subunit mass fingerprinting of mitochondrial complex I, Biochim. Biophys. Acta 1777 (2008) 1384–1391.
[6] G. Hofhaus, H. Weiss, K. Leonard, Electron microscopic analysis of the peripheral and membrane parts of mitochondrial NADH dehydrogenase (complex I), J. Mol. Biol. 221 (1991) 1027–1043.
[7] V. Guenebaut, A. Schlitt, H. Weiss, K. Leonard, T. Friedrich, Consistent structure between bacterial and mitochondrial NADH:ubiquinone oxidoreductase (complex I), J. Mol. Biol. 276 (1998) 105–112.
[8] G. Peng, G. Fritzsch, V. Zickermann, H. Schägger, R. Mentele, F. Lottspeich, M. Bostina, M. Radermacher, R. Huber, K.O. Stetter, H. Michel, Isolation, characterization and electron microscopic single particle analysis of the NADH:ubiquinone oxidoreductase (complex I) from the hyperthermophilic eubacterium *Aquifex aeolicus*, Biochem. 42 (2003) 3032–3039.
[9] M. Radermacher, T. Ruiz, T. Clason, S. Benjamin, U. Brandt, V. Zickermann, The three-dimensional structure of complex I from *Yarrowia lipolytica*: a highly dynamic enzyme, J. Struct. Biol. 154 (2006) 269–279.
[10] D.J. Morgan, L.A. Sazanov, Three-dimensional structure of respiratory complex I from *Escherichia coli* in ice in the presence of nucleotides, Biochim. Biophys. Acta 1777 (2008) 711–718.
[11] M. Finel, J.M. Skehel, S.P.J. Albracht, I.M. Fearnley, J.E. Walker, Resolution of NADH:ubiquinone oxidoreductase from bovine heart mitochondria into two subcomplexes, one of which contains the redox centers of the enzyme, Biochem. 31 (1992) 11425–11434.
[12] T. Ohnishi, Iron–sulfur clusters semiquinones in complex I, Biochim. Biophys. Acta 1364 (1998) 186–206.
[13] T. Rasmussen, D. Scheide, B. Brors, L. Kintscher, H. Weiss, T. Friedrich, Identification of two tetranuclear FeS clusters on the ferredoxin-type subunit of NADH:ubiquinone oxidoreductase (complex I), Biochem. 40 (2001) 6124–6131.
[14] L.A. Sazanov, P. Hinchliffe, Structure of the hydrophilic domain of respiratory complex I from *Thermus thermophilus*, Science 311 (2006) 1430–1436.
[15] J. Carroll, I.M. Fearnley, J.E. Walker, Definition of the mitochondrial proteome by measurement of molecular masses of membrane proteins, Proc. Natl. Acad. Sci. USA 103 (2006) 16170–16175.
[16] M.K.F. Wikström, Two protons are pumped from the mitochondrial matrix per electron transferred between NADH and ubiquinone, FEBS Lett. 169 (1984) 300–304.
[17] A.S. Galkin, V.G. Grivennikova, A.D. Vinogradov, $H^+/2^-$ stoichiometry in NADH-quinone reductase reactions catalyzed by bovine heart submitochondrial particles, FEBS Lett. 451 (1999) 157–161.
[18] K. Zwicker, A. Galkin, S. Dröse, L. Grgic, S. Kerscher, U. Brandt, The redox-Bohr group associated with iron–sulfur cluster N2 of complex I, J. Biol. Chem. 281 (2006) 23013–23017.
[19] M.L. Verkhovskaya, N. Belevich, L. Euro, M. Wikström, M.I. Verkhovsky, Real-time electron transfer in respiratory complex I, Proc. Natl. Acad. Sci. USA 105 (2008) 3763–3767.
[20] N. Kashani-Poor, K. Zwicker, S. Kerscher, U. Brandt, A central functional role for the 49-kDa subunit within the catalytic core of mitochondrial complex I, J. Biol. Chem. 276 (2001) 24082–24087.
[21] S. Kerscher, N. Kashani-Poor, K. Zwicker, V. Zickermann, U. Brandt, Exploring the catalytic core of complex I by *Yarrowia lipolytica* yeast genetics, J. Bioenerg. Biomembr. 33 (2001) 187–196.
[22] R. Böhm, M. Sauter, A. Böck, Nucleotide sequence and expression of an operon in *Escherichia coli* coding for formate hydrogenlyase components, Mol. Microbiol. 4 (1990) 231–243.
[23] S.P.J. Albracht, Intimate relationships of the large and the small subunits of all nickel hydrogenases with two nuclear-encoded subunits of mitochondrial NADH: ubiquinone oxidoreductase, Biochim. Biophys. Acta 1144 (1993) 221–224.
[24] E. Darrouzet, A. Dupuis, Genetic evidence for the existence of two quinone related inhibitor binding sites in NADH-CoQ reductase, Biochim. Biophys. Acta 1319 (1997) 1–4.
[25] E. Darrouzet, J.P. Issartel, J. Lunardi, A. Dupuis, The 49-kDa subunit of NADH-ubiquinone oxidoreductase (complex I) is involved in the binding of piericidin and rotenone, two quinone-related inhibitors, FEBS Lett. 431 (1998) 34–38.
[26] P. Ahlers, K. Zwicker, S. Kerscher, U. Brandt, Function of conserved acidic residues in the PSST-homologue of complex I (NADH:ubiquinone oxidoreductase) from *Yarrowia lipolytica*, J. Biol. Chem. 275 (2000) 23577–23582.
[27] I. Prieur, J. Lunardi, A. Dupuis, Evidence for a quinone binding site close to the interface between NUOD and NUOB subunits of complex I, Biochim. Biophys. Acta — Bioenerg. 1504 (2001) 173–178.
[28] J. Loeffen, O. Elpeleg, J. Smeitink, R. Smeets, S. Stöckler-Ipsiroglu, H. Mandel, R. Sengers, F. Trijbels, L. Van den Heuvel, Mutations in the complex I *NDUFS2* gene of patients with cardiomyopathy and encephalomyopathy, Ann. Neurol. 49 (2001) 195–201.
[29] S.D. Mills, W. Yang, K. McCormack, Molecular characterization of benzimidazole resistance in *Helicobacter pylori*, Antimicrob. Agents Chemother. 48 (2004) 2524–2530.
[30] F. Schuler, T. Yano, S. Di Bernardo, T. Yagi, V. Yankovskaya, T.P. Singer, J.E. Casida, NADH-quinone oxidoreductase: PSST subunit couples electron transfer from iron–sulfur cluster N2 to quinone, Proc. Natl. Acad. Sci. USA 96 (1999) 4149–4153.
[31] A. Garofano, K. Zwicker, S. Kerscher, P. Okun, U. Brandt, Two aspartic acid residues in the PSST-homologous NUKM subunit of complex I from *Yarrowia lipolytica* are essential for catalytic activity, J. Biol. Chem. 278 (2003) 42435–42440.
[32] L. Grgic, K. Zwicker, N. Kashani-Poor, S. Kerscher, U. Brandt, Functional significance of conserved histidines and arginines in the 49 kDa subunit of mitochondrial complex I, J. Biol. Chem. 279 (2004) 21193–21199.
[33] S. Kerscher, V. Zickermann, K. Zwicker, U. Brandt, Insights into the mechanism of mitochondrial complex I from its distant relatives, the [NiFe] hydrogenases, in: M. Wikstrom (Ed.), Biophysical and Structural Aspects of Bioenergetics, RSC Publishing, Cambridge, 2005, pp. 156–184.
[34] N. Ichimaru, M. Murai, N. Kakutani, J. Kako, A. Ishihara, Y. Nakagawa, T. Nishioka, T. Yagi, H. Miyoshi, Synthesis and characterization of new piperazine-type inhibitors for mitochondrial NADH-ubiquinone oxidoreductase (complex I), Biochem. 47 (2008) 10816–10826.
[35] M.A. Tocilescu, U. Fendel, K. Zwicker, S. Kerscher, U. Brandt, Exploring the ubiquinone binding cavity of respiratory complex I, J. Biol. Chem. 282 (2007) 29514–29520.

[36] U. Fendel, M.A. Tocilescu, S. Kerscher, U. Brandt, Exploring the inhibitor binding pocket of respiratory complex I, Biochim. Biophys. Acta 1777 (2008) 660–665.
[37] M. Degli Esposti, Inhibitors of NADH-ubiquinone reductase: an overview, Biochim. Biophys. Acta 1364 (1998) 222–235.
[38] J.G. Okun, P. Lümmen, U. Brandt, Three classes of inhibitors share a common binding domain in mitochondrial complex I (NADH:ubiquinone oxidoreductase), J. Biol. Chem. 274 (1999) 2625–2630.
[39] A. Eschemann, A. Galkin, W. Oettmeier, U. Brandt, S. Kerscher, HDQ (1-Hydroxy-2-dodecyl-4(1*H*)quinolone), a high affinity inhibitor for mitochondrial alternative NADH dehydrogenase, J. Biol. Chem. 280 (2005) 3138–3142.
[40] I. Wittig, H.P. Braun, H. Schägger, Blue native PAGE, Nat. Protoc. 1 (2006) 418–428.
[41] N. Kashani-Poor, S. Kerscher, V. Zickermann, U. Brandt, Efficient large scale purification of his-tagged proton translocating NADH:ubiquinone oxidoreductase (complex I) from the strictly aerobic yeast *Yarrowia lipolytica*, Biochim. Biophys. Acta 1504 (2001) 363–370.
[42] S. Dröse, A. Galkin, U. Brandt, Proton pumping by complex I (NADH:ubiquinone oxidoreductase) from *Yarrowia lipolytica* reconstituted into proteoliposomes, Biochim. Biophys. Acta 1710 (2005) 87–95.
[43] S. Dröse, A. Galkin, U. Brandt, Measurement of superoxide formation by mitochondrial complex I of *Yarrowia lipolytica*, Meth. Enzymol. 456 (2009) 475–490.
[44] F. Di Virgilio, G.F. Azzone, Activation of site I redox-driven H+ pump by exogenous quinones in intact mitochondria, J. Biol. Chem. 257 (1982) 4106–4113.
[45] E. Estornell, R. Fato, F. Pallotti, G. Lenaz, Assay conditions for the mitochondrial NADH:coenzyme Q oxidoreductase, FEBS Lett. 332 (1993) 127–131.
[46] R. Fato, E. Estornell, S. Di Bernardo, F. Pallotti, G.P. Castelli, G. Lenaz, Steady-state kinetics of the reduction of coenzyme Q analogs by complex I (NADH:ubiquinone oxidoreductase) in bovine heart mitochondria and submitochondrial particles, Biochem. 35 (1996) 2705–2716.
[47] G. Lenaz, Quinone specificity of complex I, Biochim. Biophys. Acta 1364 (1998) 207–221.
[48] N. Hano, Y. Nakashima, K. Shinzawa-Itoh, S. Yoshikawa, Effect of the side chain structure of coenzyme Q on the steady state kinetics of bovine heart NADH: coenzyme Q oxidoreductase, J. Bioenerg. Biomembr. 35 (2003) 257–265.
[49] V. Zickermann, B. Barquera, M.K.F. Wikström, M. Finel, Analysis of the pathogenic human mitochondrial mutation ND1/3460, and mutations of strictly conserved residues in its vicinity, using the bacterium *Paracoccus denitrificans*, Biochem. 37 (1998) 11792–11796.
[50] S. Kurki, V. Zickermann, M. Kervinen, I.E. Hassinen, M. Finel, Mutagenesis of three conserved Glu residues in a bacterial homologue of the ND1 subunit of complex I affects ubiquinone reduction kinetics but not inhibition by dicyclohexylcarbodiimide, Biochem. 39 (2000) 13496–13502.
[51] K. Sakamoto, H. Miyoshi, M. Ohshima, K. Kuwabara, K. Kano, T. Akagi, T. Mogi, H. Iwamura, Role of the isoprenyl tail of ubiquinone in reaction with respiratory enzymes: studies with bovine heart mitochondrial complex I and *Escherichia coli bo*-type ubiquinol oxidase, Biochem. 37 (1998) 15106–15113.
[52] J.M. Berrisford, L.A. Sazanov, Structural basis for the mechanism of respiratory complex I, J. Biol. Chem. 284 (2009) 29773–29783.